Glaucoma Specialist Detection of Optical Coherence Tomography Suspicious Rim Tissue in Glaucoma and Glaucoma Suspect Eyes

SEUNG WOO HONG, HELEN KOENIGSMAN, HONGLI YANG, RUOJIN REN, JUAN REYNAUD, ROBERT M. KINAST, STEVEN L. MANSBERGER, BRAD FORTUNE, SHABAN DEMIREL, STUART K. GARDINER, AND CLAUDE F. BURGOYNE

• PURPOSE: To assess glaucoma specialists' detection of optic nerve head (ONH) rim tissue that is thin by optical coherence tomography (OCT) criteria.

• DESIGN: Reliability analysis.

• METHODS: Five clinicians marked the disc margin (DM) and rim margin (RM) on stereophotographs of 151 glaucoma or glaucoma suspect eyes obtained within 3 months of OCT imaging. The photo and OCT infrared image for each eye were co-localized and regionalized into 12 sectors relative to the axis between the Bruch membrane opening (BMO) centroid and the fovea. For each clinician, the distance from BMO centroid to their DM (DM radius) and RM (RM radius) was used to generate sectoral rim width (RW) (DM radius–RM radius) and cup-to-disc ratio (CDR) (RM radius/DM radius) estimates. OCT minimum rim width (MRW) was determined by sector. Among all eyes, for each OCT MRW suspicious sector (<5% of OCT normative database), we determined each clinician's detection (clinician CDR ≥ 0.7).

• RESULTS: Clinicians most commonly failed to detect OCT suspicious rim tissue in the nasal sectors. Among 502 sectors with suspicious OCT MRW, all 5 clinicians rated CDR ≥ 0.7 in only 29.5% and all 5 clinicians rated CDR < 0.7 in 21%. OCT suspicious rim thickness was most common (32% of eyes) in the nasal and inferior sectors. MRW vs clinician RW discordance was greatest nasally, while BMO vs clinician DM discordance was greatest temporally.

• CONCLUSIONS: Clinicians most commonly failed to detect OCT suspicious rim thickness nasally where suspicious rim tissues were also most common. (Am J Ophthalmol 2019;199:28–43. © 2018 Elsevier Inc. All rights reserved.)

AJO.com Supplemental Material available at AJO.com.

Accepted for publication Oct 26, 2018.

From the Optic Nerve Head Research Laboratory (S.W.H., H.K., H.Y., R.R., J.R., C.F.B.) and Discoveries in Sight Research Laboratories (J.R., S.L.M., B.F., S.D., S.K.G., C.F.B.), Devers Eye Institute, Legacy Research Institute, Portland, Oregon, USA; Devers Eye Institute Glaucoma Service, Portland, Oregon, USA (R.M.K., S.L.M., C.F.B.); and Department of Ophthalmology, Medical College, the Catholic University of Korea, Seoul, South Korea (S.W.H.).

Inquiries to Claude F. Burgoyne, Optic Nerve Head Research Laboratory, Devers Eye Institute, Legacy Research Institute, 1225 NE 2nd Ave, Portland, OR 97208-3950 USA; e-mail: cfburgoyne@deverseye.org

CLINICIAN VARIABILITY IN THE CLINICAL DISC examination is well documented,[1–5] but until recently[6] glaucoma specialists' disc margin, rim margin, and rim width variability had not been rigorously assessed. In a previous report,[6] we asked 5 glaucoma specialists to independently, digitally delineate the disc margin and rim margin (Figure 1, Top row), within optic disc stereophotographs from 1 eye each of 214 glaucoma or glaucoma suspect eyes. Each stereophotograph was then co-localized to the infrared (IR) fundus image obtained by optical coherence tomography (OCT) scan, enabling optic nerve head (ONH) 30-degree (clock-hour) sectors to be consistently imposed upon each eye, based on the position of the fovea relative to the center of the ONH (Figure 1, Bottom left).[7] We found disc margin, rim margin, rim width, and cup-to-disc ratio (CDR) (Figure 1, Bottom right) discordance among the 5 clinicians to be substantial and common in sectors that were suspicious for rim thinning.

In the present report, we compare each clinician's rim width estimate to co-localized OCT minimum rim width (MRW) measurements,[8] within a subset of 151 eyes from our previous study,[6] so as to assess their ability to detect sectors in which the rim tissue was thin by OCT MRW criteria (<5th percentile of an OCT MRW normative database [NDB]).[9] While a clinician's rim width estimate is not directly comparable to an OCT MRW measurement owing to anatomic and geometric considerations[10] (Figure 2), assessing clinicians' ability to detect rim tissues that are thin by OCT MRW criteria is important because a clinician must be suspicious enough, based on his or her own clinical examination, to decide that subsequent OCT imaging and/or functional testing is required.

To date, no study has objectively assessed clinicians' ability to sectorally detect rim tissues that are suspicious for being thin by OCT criteria. Specifically assessing clinicians' ability to sectorally detect rim tissues that are within the thinnest 5th percentile of a robust OCT database[9] is additionally important because this criterion has been used to detect glaucoma[11,12] at levels of sensitivity (at 95% specificity) that are higher than those usually achieved by individual clinicians.[13,14]

0002-9394/$36.00
https://doi.org/10.1016/j.ajo.2018.10.027

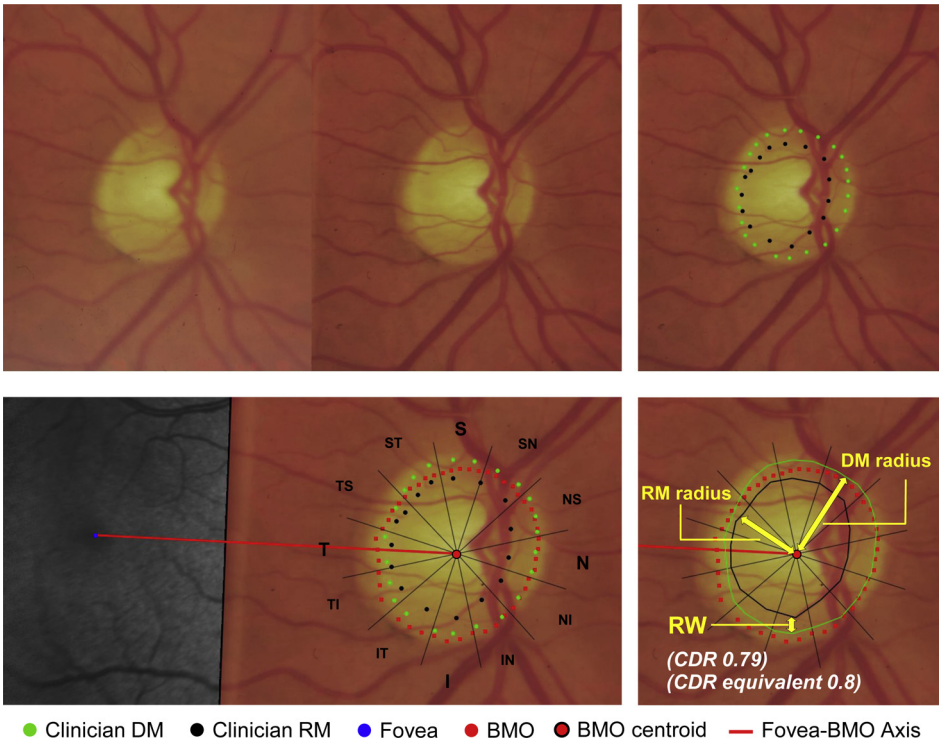

FIGURE 1. Clinician disc margin (DM) radius, rim margin (RM) radius, and rim width (RW) measurements in each study eye.[6] A stereophotograph of each optic nerve head (ONH) (Top left) was individually viewed by each clinician while simultaneously marking the DM (green dots) and RM (black dots), within the best focused image of the stereo-pair (Top right), viewed within custom marking software on an adjacent monitor. (Bottom left) After co-localization of each disc photograph to the infrared fundus reflectance image of the paired optical coherence tomography (OCT) data set, a line connecting the Bruch membrane opening (BMO) centroid (red dot) and the foveal center (blue dot) was drawn to establish the foveal-BMO (FoBMO) axis (red line), which was then used as the horizontal axis for 12 30-degree (clock hour) sectors (black borders). (Bottom right) After connecting the DM and RM points of each clinician by straight lines (DM, green; RM, black), a single measurement of DM radius, RM radius, and RW (DM radius–RM radius) was made along the midline of the sector, relative to the BMO centroid. Cup-to-disc ratio (CDR) was calculated as RM radius/DM radius, and CDR equivalent was defined to be the CDR rounded to the nearest single decimal place. All CDR data in this report are CDR equivalents to most closely mimic clinical practice. Throughout the text the 12 FoBMO sectors shown in the bottom left panel are italicized when referred to individually: (S) *superior*; (SN) *superior-nasal*; (NS) *nasal-superior*; (N) *nasal*; (NI) *nasal-inferior*; (IN) *inferior-nasal*; (I) *inferior*; (IT) *inferior-temporal*; (TI) *temporal-inferior*; (T) *temporal*; (TS) *temporal-superior*; (ST) *superior-temporal*. Note that while it is most common for the fovea to be "below" the acquired image frame (AIF) horizontal axis,[7] in this eye, likely owing to cyclotorsion and/or head tilt during imaging, the fovea is above the AIF horizontal axis of the disc. Linking ONH sectoral regionalization to retinal anatomy (the FoBMO axis), instead of the AIF horizontal axis, ensures that ONH regionalization is not affected by cyclotorsion and/or head tilt.[7]

SUBJECTS AND METHODS

• **BACKGROUND AND DEMOGRAPHICS:** This study was performed on photographs and OCT data sets from 151 of the 214 individuals in our previous report[6] who met the OCT imaging criteria outlined below. All were participants in the Portland Progression Project,[15] a National Institutes of Health–funded, longitudinal study of progression in high-risk ocular hypertension and glaucoma that is based at the Legacy Devers Eye Institute in Portland, Oregon, USA. The protocol was approved and monitored by the Legacy Health Institutional Review Board. The study adheres to the tenets of the Declaration of Helsinki and complies with the Health Insurance Portability and Accountability Act of 1996. All participants provided written informed consent, after having the risks and benefits of participation explained to them.

Study participants[15] had best-corrected vision ≥20/40 and 1 or more of the following risk factors for glaucoma progression: age >70, systemic hypertension, migraine, diet-controlled diabetes, peripheral vasospasm, African ancestry, or family history of glaucoma. Participants with ocular, neurologic, or systemic diseases; medications that can affect the visual field; or previous ocular trauma including ocular surgery (except for uncomplicated cataract surgery) were excluded. Each subject underwent pachymetry, stereophotography, OCT ONH and retinal nerve fiber layer (RNFL) imaging, and visual field testing.

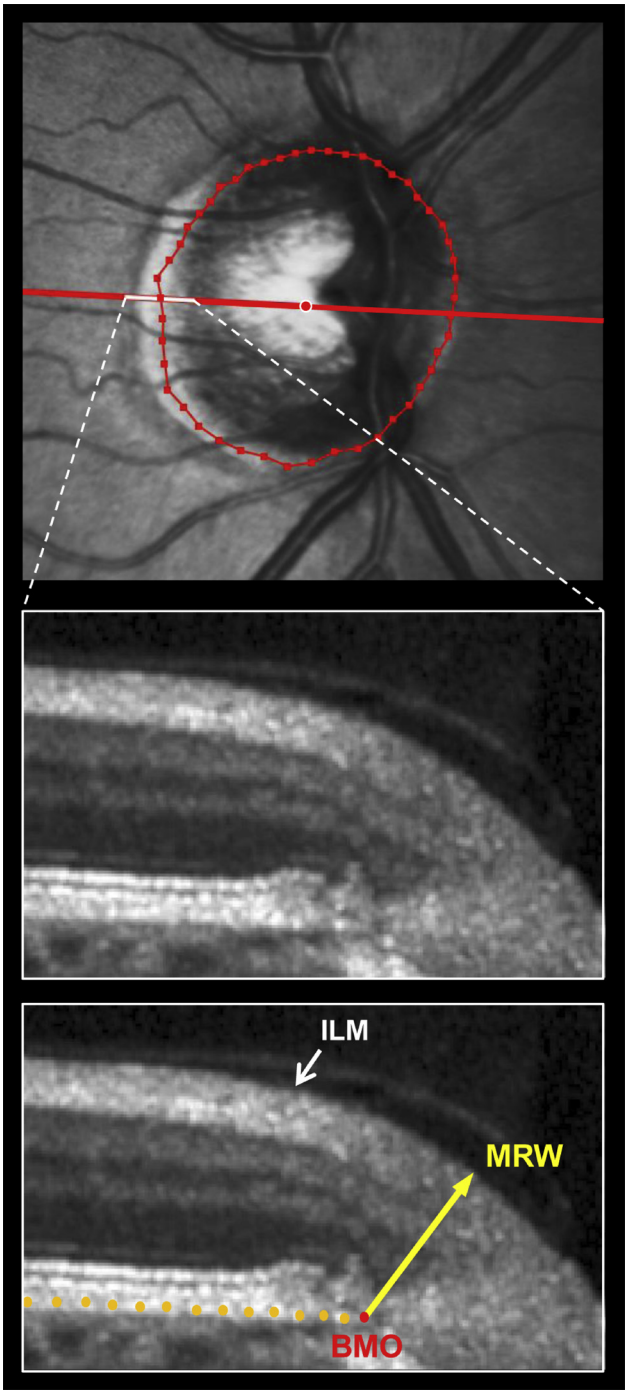

FIGURE 2. Optical coherence tomography (OCT) Bruch membrane opening (BMO) minimum rim width (MRW). (Top) OCT BMO points (red dots) and the location of the foveal-BMO (FoBMO) axis B-scan (red line) has been projected onto the infrared reflectance image of the OCT data set. (Center) The portion of the FoBMO axis B-scan shown in white in the top panel. (Bottom) Bruch membrane (BM, orange dots), BMO (red dot), and BMO-MRW (yellow arrow) are shown. BMO-MRW is defined to be the shortest distance between BMO and the internal limiting membrane (ILM). Because OCT MRW measurements are a 3-dimensional "minimum thickness" measurement and the clinician rim width estimate, of necessity is made within the plane of the retina, OCT MRW is not directly comparable to clinician rim width (see Figure 10 for more details).

• **IMAGING:** Only subjects with ONH photography and OCT imaging performed within 3 months of each other were included in this study. ONH stereophotographs were obtained using a simultaneous stereoscopic camera (3-Dx; Nidek Co Ltd, Gamagori, Japan) after maximum pupil dilation. The images were acquired on 35-mm slide film, developed and processed into color slides. The slides were digitized with a slide scanner (Nikon LS-5000 ED; Nikon Corporation, Tokyo, Japan) at a resolution of 4800 dpi. OCT imaging (Spectralis; Heidelberg Engineering GmbH, Heidelberg, Germany), included a 30-degree infrared fundus image of the posterior pole including the ONH and fovea (using the integrated confocal scanning laser ophthalmoscope), and a 24 radial B-scan data set (each B-scan was 15 degrees wide, contained 768 A-scans, and was the average of 9 repetitions).

One eye of each subject was randomly selected for analysis. For each study eye, the illumination and focus of the left and right images of the stereoscopic image pair were qualitatively compared and the best was chosen for simultaneous digital delineation of the disc and rim margins, as outlined below (Figure 1).

• **CLINICIAN DISC MARGIN NND RIM MARGIN ASSESSMENT WITHIN EACH STEREOPHOTOGRAPH:** Five glaucoma specialists independently viewed the stereophotograph pairs of each study eye using a stereoscopic viewer (Screen Vu; PS Manufacturing, Portland, Oregon, USA) on a computer monitor without instructions as to how to mark the disc margin and rim margin points or awareness of the other clinicians' marks (Figure 1, Top left). The clinical training and years of experience as a glaucoma specialist for the 5 clinicians ranged from 0 to 19 years. The disc margin and rim margin points of each examiner were digitally "burned" onto a separate copy of the better-focused image of the stereophotograph pair, using a second adjacent monitor and custom software (Figure 1, Top right). The purpose of this exercise was to document clinician variability in disc and rim margin assignment. Clinicians were not asked to assess if the rim tissue was abnormally thin, nor were they told their derived rim widths would be compared to OCT MRW measurements.

• **CLINICIAN-SPECIFIC DISC MARGIN, RIM MARGIN, RIM WIDTH, AND CUP-TO-DISC RATIO MEASUREMENTS WITHIN THE STEREOPHOTOGRAPH OF EACH STUDY EYE:** For each study eye, the delineated Bruch membrane opening (BMO) points and the BMO centroid from its ONH OCT data set (Figure 1, Bottom left, and Figure 2, Top,

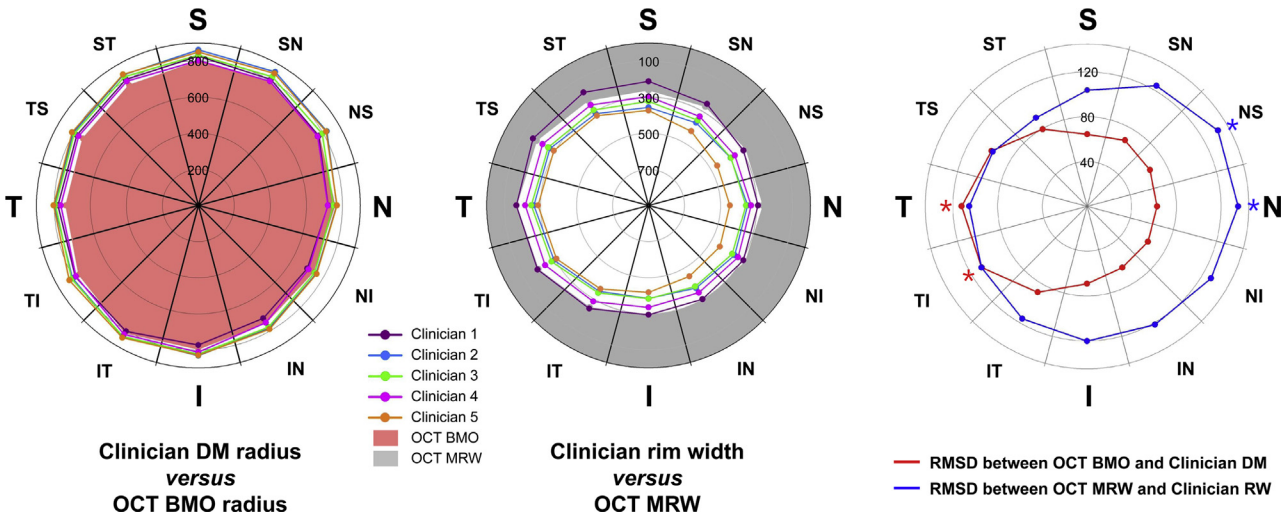

FIGURE 3. Polar plots of the sectoral mean values for each clinician's disc margin (DM) radius vs optical coherence tomography (OCT) Bruch membrane opening (BMO) radius (solid red) (Left) and clinician's rim width (RW) vs the mean OCT minimum rim width (MRW, solid gray) (Center) across all 151 study eyes and the sectoral discordance (root mean square differences between OCT BMO and clinicians' disc margin (DM) radius (red), as well as OCT MRW and clinicians' rim width (RW) (blue) (Right). Data are in micrometers. (Left) Note that the mean OCT BMO radius is less than the mean DM radius of most clinicians within most sectors, suggesting that OCT BMO lies inside of the clinically visible disc margin in most sectors of most eyes relative to the center of BMO. (Center) The mean rim width for 4 of the 5 clinicians falls inside of (ie, is greater than) the mean OCT MRW in all sectors ($P < .001$ by Wilcoxon test). Clinician 1's mean rim width overlies the mean OCT MRW in all sectors except in the superior and superior temporal sectors, where it is smaller than OCT MRW ($P < .001$ by Wilcoxon test). (Right) Discordance between BMO and the clinicians' DM was greatest in the temporal sectors (red stars, T and TI, $P < .001$ by Wilcoxon test), whereas discordance between OCT MRW and clinicians' RW was greatest in the nasal sectors (blue stars, NS and N, $P \leq .003$ by Wilcoxon test). See Figure 1 for sectoral nomenclature.

and further explained in OCT methods below) were projected onto the OCT infrared fundus image, wherein the axis between the BMO centroid and the fovea (the FoBMO axis) was established. The boundaries of each FoBMO 30-degree ("clock-hour") sector were then defined relative to this axis (Figure 1, Bottom left). Thus, a common set of retinal and ONH anatomic landmarks were employed to consistently define the position of the 30-degree FoBMO ONH sectors in each study eye, rather than using the orientation of the fundus relative to the horizontal axis of the acquired image frame, which can vary from eye to eye.[7] The disc margin and rim margin points for each clinician (Figure 1, Bottom left) were co-localized to the OCT IR fundus image (Figure 1, Bottom left), using a previously described technique[16] performed within Image J (version 1.43u, TurboReg plug-in; National Institutes of Health, Bethesda, Maryland, USA).

Within each photograph, each clinician's disc margin and rim margin points were connected and a single sectoral measurement of disc margin radius, rim margin radius, and rim width (disc margin radius–rim margin radius) were made from the BMO centroid along the centerline of each 30-degree sector (Figure 1, Bottom right). Sectoral CDR equivalents for each clinician were then calculated as follows: sectoral rim margin radius/disc margin radius (rounded to a single decimal place to mimic clinical practice). All left-eye data were converted into right-eye orientation.[17]

• **OPTICAL COHERENCE TOMOGRAPHY MINIMUM RIM WIDTH MEASUREMENTS BY BRUCH MEMBRANE OPENING CENTROID AND FOVEA 30-DEGREE SECTORS:** BMO was manually segmented within each of the 24 ONH radial B-scans for each eye, and OCT MRW was calculated as the minimum distance between BMO and the internal limiting membrane (ILM) (Figure 2), as previously described.[8] Sectoral values for MRW were derived from 48 equally spaced angular positions around the BMO centroid, with the 12 sectoral mean MRW measurements being the average of 4 MRW measurements per sector.

• **DATA ANALYSIS:** The experiment-wide (n = 151 eyes) mean disc margin radius, rim margin radius, and rim width were calculated for each clinician by sector. For each eye, the root mean square difference (RMSD) between the BMO radius and the disc margin radii of the 5 clinicians, as well as the RMSD between OCT MRW and the rim widths of the 5 clinicians, was calculated for each sector. The statistical significance of intersectoral differences in the RMSDs across all 151 study eyes was assessed for each comparison by Wilcoxon test.

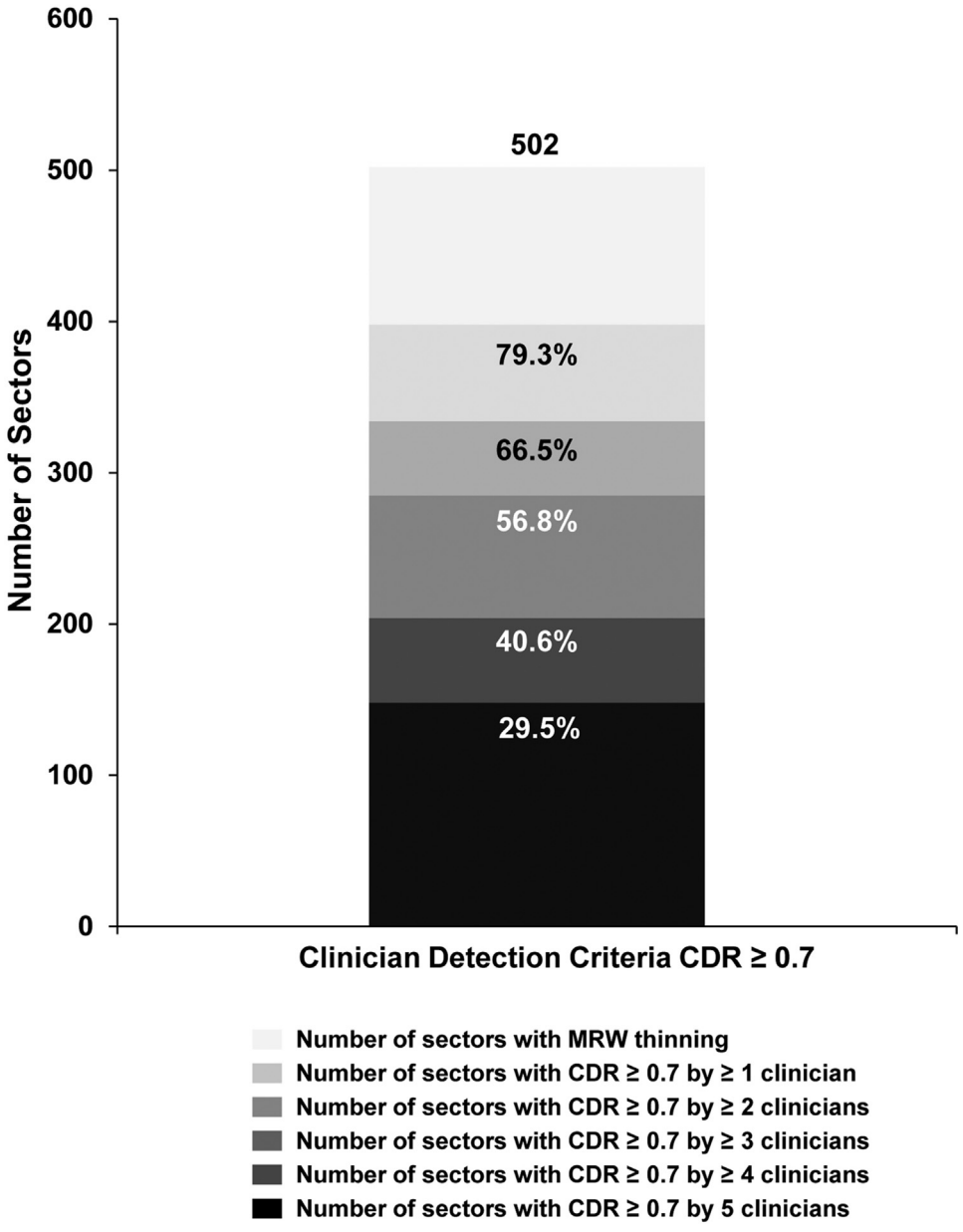

FIGURE 4. Frequency of clinician rim thinning detection using cup-to-disc ratio (CDR) criteria ≥ 0.7 within optical coherence tomography (OCT) *suspicious* sectors. The number at the top of the column is the number of sectors, among all 1812 (151 × 12) study eye sectors, in which OCT minimum rim width (MRW) was suspicious (< the 5th percentile of the OCT MRW normative database). White or black numbers at the top of each shade of gray are the number of suspicious sectors (expressed in percent) in which the given number of clinicians' CDR was ≥0.7. The white number at the top of the black portion of the column is the number of suspicious sectors (expressed in percent) in which all 5 clinicians' CDR was ≥0.7 (29.5%).

To assess the clinicians' ability to detect ONH sectors that were thin by OCT criteria, we first identified all sectors in which the sectoral MRW value (after being corrected for age and BMO area)[9] was less than the 5th percentile of the OCT Caucasian NDB.[9] We then assessed clinician "detection" of these sectors using 2 definitions of detection: a sectoral CDR equivalent ≥ 0.6, and a sectoral CDR equivalent ≥ 0.7, based on previous studies that have used these definitions.[17–22] Finally, to estimate the rate of false-positive clinician determination of suspicious rim thinning using

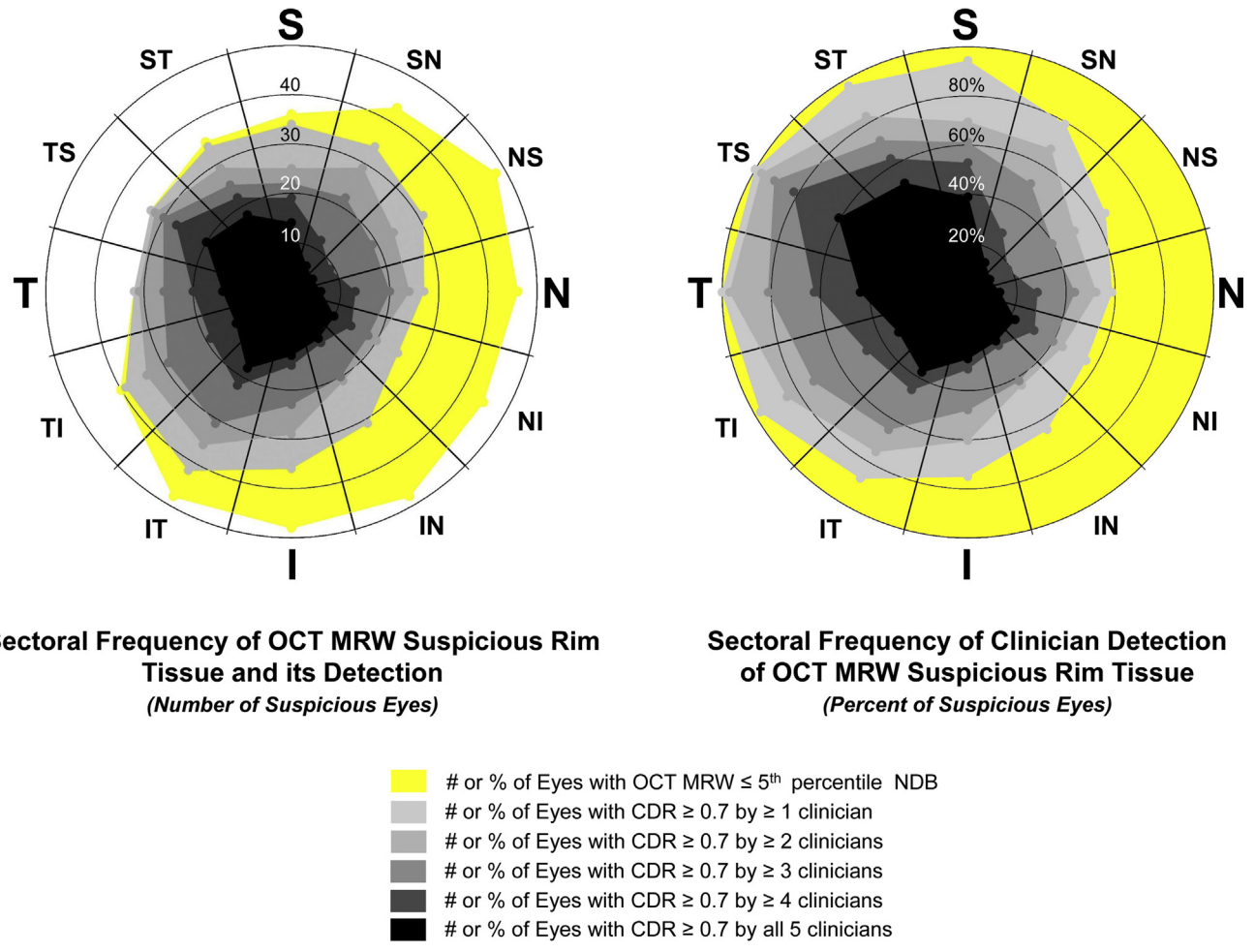

FIGURE 5. Frequency of optical coherence tomography (OCT) minimum rim width (MRW) "*suspicious*" rim tissue among the 151 study eyes by fovea–Bruch membrane opening (FoBMO) sector and the frequency and agreement of its detection by clinicians using a cup-to-disc ratio (CDR) criterion of ≥0.7. (Left) The outermost area (yellow) represents the number of study eyes in which OCT MRW is *suspicious* (< the 5th percentile of the normative database) for each sector. Each shade of gray represents the number of suspicious eyes in which the corresponding number of clinicians' CDR was ≥0.7 (ie, their agreement). (Right) The outermost yellow area denotes 100% of the suspicious eyes in each sector. Each shade of gray represents the percentage of suspicious eyes in which the corresponding number of clinicians' CDR was ≥0.7 (ie, their agreement). Taken together, these data suggest that while the frequency of OCT MRW suspicious rim tissue was greatest within the nasal and inferior sectors, clinician detection of OCT MRW suspicious rim tissue was lowest in the nasal sectors and greatest within the superior temporal sectors at all levels of clinician agreement.

each detection definition, we assessed their performance within "normal" sectors, using 2 OCT MRW definitions of "normal" (≥5th percentile and ≥10th percentile of the NDB, respectively).

A χ^2 test was used to assess the statistical significance of sectoral differences in the frequency of clinician detection of rim tissue that was suspicious by OCT MRW criteria, as well as differences in the frequency of false-positive detection of suspicious rim thickness in sectors that were "normal" by OCT criteria.

RESULTS

THIS STUDY INCLUDED 151 EYES OF 151 SUBJECTS RANGING in age from 33 to 89 years (mean ± standard deviation

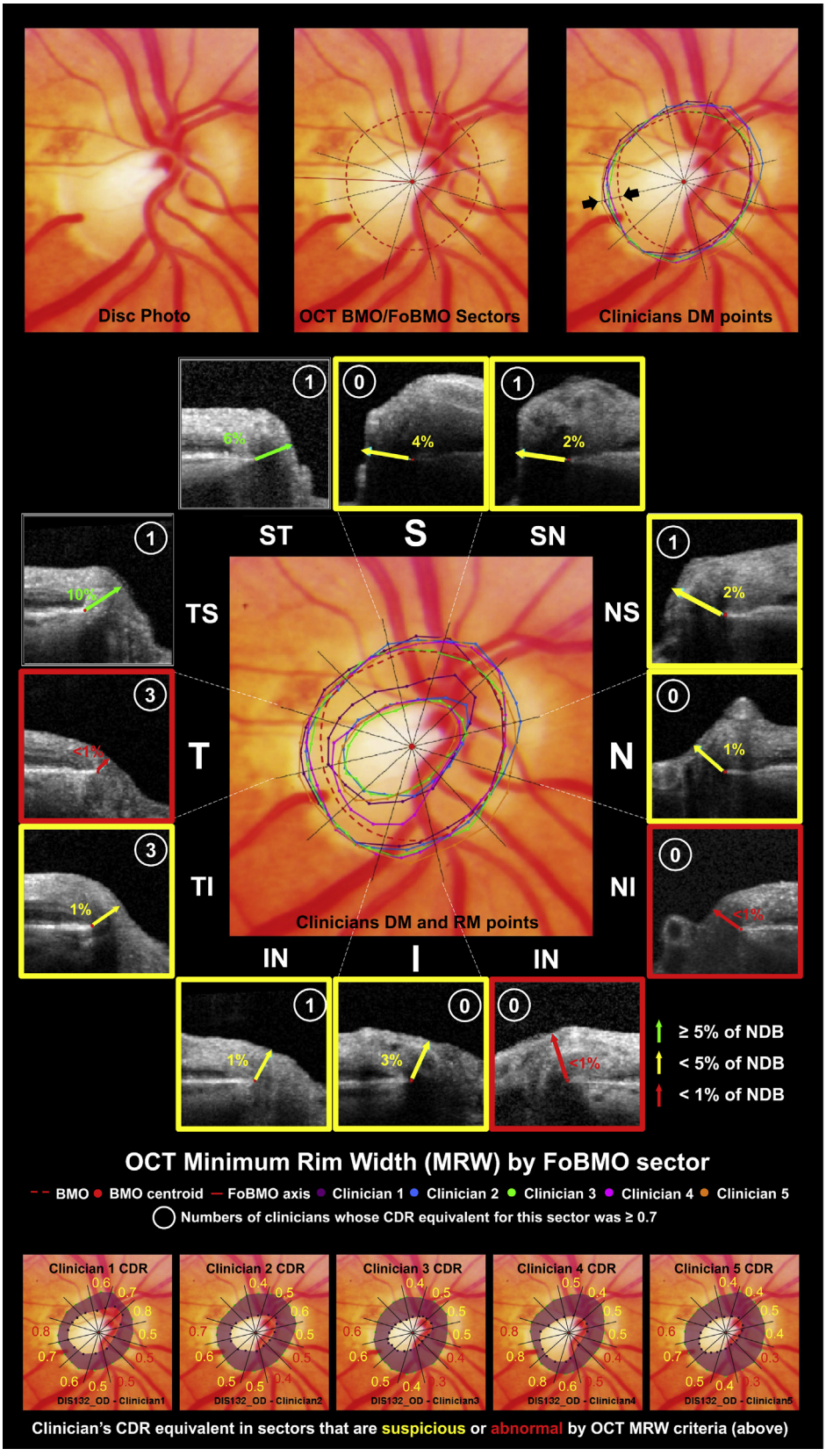
Disc Photo
OCT BMO/FoBMO Sectors
Clinicians DM points
ST
S
SN
TS
NS
T
N
TI
NI
IN
I
IN
Clinicians DM and RM points
≥ 5% of NDB
< 5% of NDB
< 1% of NDB
OCT Minimum Rim Width (MRW) by FoBMO sector
BMO BMO centroid FoBMO axis Clinician 1 Clinician 2 Clinician 3 Clinician 4 Clinician 5
Numbers of clinicians whose CDR equivalent for this sector was ≥ 0.7
Clinician 1 CDR
Clinician 2 CDR
Clinician 3 CDR
Clinician 4 CDR
Clinician 5 CDR
Clinician's CDR equivalent in sectors that are suspicious or abnormal by OCT MRW criteria (above)

64 ± 11 years). Eighty-four (56.6%) were right eyes and the mean visual field mean deviation was -0.61 ± 2.86 decibels (range -14.97 to 2.74). Most of the participants were white (143, 94.7%) and approximately half (84, 56.6%) were female. Stereophotograph and OCT imaging were acquired on the same day in 84% of study eyes.

Each clinician's mean disc margin radius vs the mean OCT BMO radius by sector across all 151 eyes are reported in Figure 3 (Left). On average, BMO radius was smaller than the disc margin radii of all 5 clinicians within the temporal and superior sectors, and smaller than the disc margin radii of most clinicians within the nasal and inferior sectors. Among the 151 study eyes, the sectoral frequency of BMO radius being smaller than all 5 clinicians' disc margin radii ranged from 21.2% to 68.2%, being most frequent within the inferior-temporal (51.7%), temporal-inferior (64.2%), temporal (65.6%), temporal-superior (68.2%), and superior-temporal (66.9%) sectors. The frequency of BMO radius being larger than all 5 clinicians' disc margin radii ranged from 7.9% to 26.5%, being most frequent within the nasal (26.5%), nasal-inferior (23.2%), inferior-temporal (19.2%), temporal-inferior (18.5%), temporal (18.5%), and temporal-superior (14.6%) sectors. The sectoral magnitude of OCT BMO vs clinicians' disc margin radii discordance, across all 151 eyes (Figure 3, Right), was highest in the temporal and temporal-inferior sectors compared to all other sectors ($P < .001$, Wilcoxon test).

Each clinician's mean rim width vs the mean OCT MRW by sector across all 151 eyes are reported in Figure 3 (Center). The mean rim width for 4 clinicians (Clinicians 2-5) was greater than the mean OCT MRW in all sectors (Figure 3, Center). Among the 1812 study-eye sectors, the frequency of each clinicians' sectoral rim width being greater than OCT MRW was 44% for Clinician 1 and 83%, 81%, 72%, and 91% for Clinicians 2-5, respectively. The sectoral magnitude of OCT MRW vs clinician rim width discordance (Figure 3, Right) was highest in the nasal-superior and nasal sectors compared to all other sectors ($P \leq .003$).

The sectoral distribution (mean, 5th, and 95th percentiles) of the study eye OCT MRWs are reported relative to the distribution of the Caucasian NDB in Supplemental Figure 1 (Supplemental Material available at AJO.com). Among the 1812 study-eye sectors (151 eyes × 12 sectors/eye), 502 (28.7%) were suspicious, by OCT MRW criteria (Figure 4). Among the 502 suspicious sectors, all 5 clinicians' CDR equivalent was ≥0.7 in only 148 sectors (29.5%) (Figure 4) and ≥0.6 in only 290 sectors (57.8%) (Supplemental Figure 2; Supplemental Material available at AJO.com).

Suspicious OCT MRW rim thickness occurred most commonly in the nasal sectors and inferior sectors and least commonly in the temporal sectors (Figure 5). The sectoral frequency of all 5 clinicians' detecting OCT MRW suspicious rim thickness using a CDR criteria of ≥0.7 ranged from 10% to 61% (Figure 5), whereas the sectoral frequency of fewer than 3 clinicians detecting OCT MRW suspicious rim thickness using CDR ≥ 0.7 ranged from 9.0% to 60%. The frequency of detection for CDR ≥ 0.7 was greatest within the temporal sectors and least within the nasal sectors ($P < .001$, χ^2). The sectoral frequency of all 5 clinicians' detection of OCT MRW suspicious rim thickness using a CDR criterion of ≥0.6 ranged from 33% to 91% (Supplemental Figure 3; Supplemental Material available at AJO.com), whereas the sectoral frequency of fewer than 3 clinicians detecting OCT MRW suspicious rim thickness using CDR ≥ 0.6 ranged from 3% to 56%. The frequency of detection for CDR ≥ 0.6 was also greatest within the temporal sectors and least within the nasal sectors ($P < .001$, χ^2).

A representative study eye in which clinicians variably failed to detect rim tissue that was suspicious in 10 of the 12 sectors (CDR ≥ 0.7 criterion) is shown in Figure 6. A broad region in which the clinical disc margins of all 5 clinicians fell outside of BMO may have contributed to the underdiagnosis of suspicious rim tissue in the temporal sectors. Yet all 5 clinicians also failed to detect suspicious rim tissues

FIGURE 6. Clinician failure to detect nasal and temporal optical coherence tomography (OCT) minimum rim width (MRW) suspicious rim thickness in a representative study eye using a cup-to-disc ratio (CDR) ≥ 0.7 detection criterion. (Top left) Fundus photograph from study subject DIS132. (Top middle) Bruch membrane opening (BMO), the centroid of BMO, the fovea–BMO axis (FoBMO axis, red line), and the 12 FoBMO 30-degree (clock-hour) sectors (black lines) (Top right) BMO relative to the disc margin points of all 5 clinicians. Note that BMO is well inside the clinical disc margin points of all 5 clinicians temporally (black arrows), suggesting that BMO was clinically invisible to these clinicians in this region.[10,23] (Center panels) BMO and each clinician's disc margin and rim margin points have been superimposed on the fundus photograph in the center, and OCT rim anatomy along with its quantification relative to a Caucasian normative database (NDB) are shown for each FoBMO sector. Note that the OCT anatomy boxes have been outlined in yellow and red when the OCT MRW anatomy (yellow or red arrow) is < the 5th percentile or < the 1st percentile of the NDB. While our study treats all sectors < 5th percentile of the NDB as suspicious, we include the red distinction to be consistent with several clinical imaging devices. In a white circle at the top of each OCT anatomy box, the number of clinicians that were suspicious for rim thinning by the CDR ≥ 0.7 criterion are noted. (Bottom row) Each clinician's rim width (purple) and their CDR equivalent for the OCT MRW *suspicious* sectors of interest are shown. Note that while the clinicians' rim width and CDRs are relatively concordant, within the inferior-nasal sectors, none of the 5 clinicians was suspicious for rim thinning by the CDR ≥ 0.7 criterion. See Figure 10 for a more detailed discussion of the *temporal-inferior* (IT) and *inferior-nasal* (IN) sectoral anatomy.

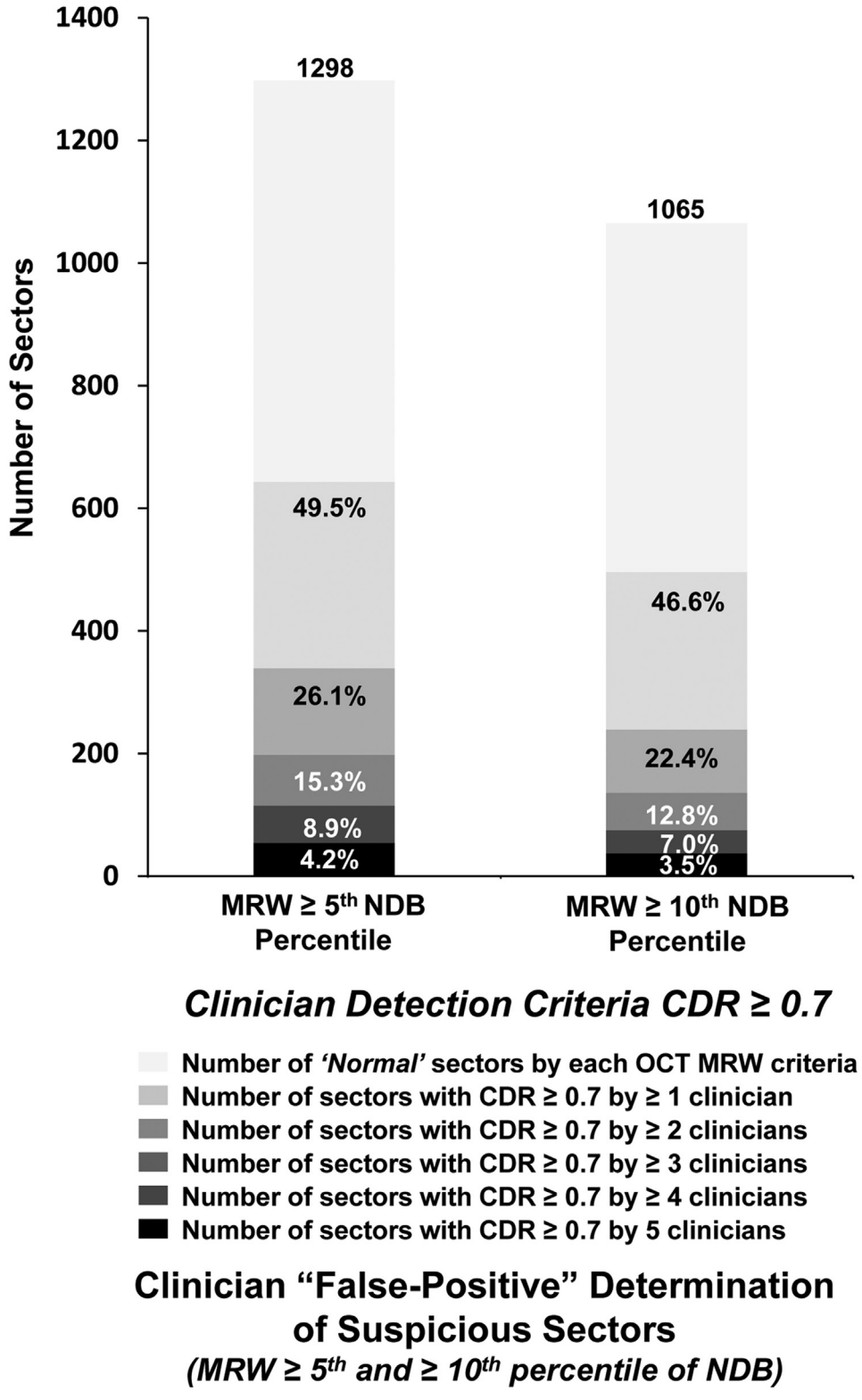

FIGURE 7. Frequency of *false-positive* rim thinning determination by clinicians using the criterion cup-to-disc ratio (CDR) ≥ 0.7 within optical coherence tomography (OCT) minimum rim width (MRW) "normal" sectors defined using 2 definitions of normal. (Left column) OCT MRW ≥ the lowest 5th percentile of the OCT MRW normative database (NDB) and (right column) OCT MRW ≥ the lowest 10th percentile of the NDB. Black numbers at the top of each column are the number of sectors (among all 1812 [151 × 12] study eye sectors) in which OCT MRW was "*normal*" by the specific MRW criteria. Within each column, white or black numbers at the top of each shade of gray are the number of normal sectors (expressed in percent) in which the given number of clinicians' CDR was ≥0.7. White numbers at the top of the black portion of the columns are the number of normal sectors (expressed in percent) in which all 5 clinicians' CDR was ≥0.7.

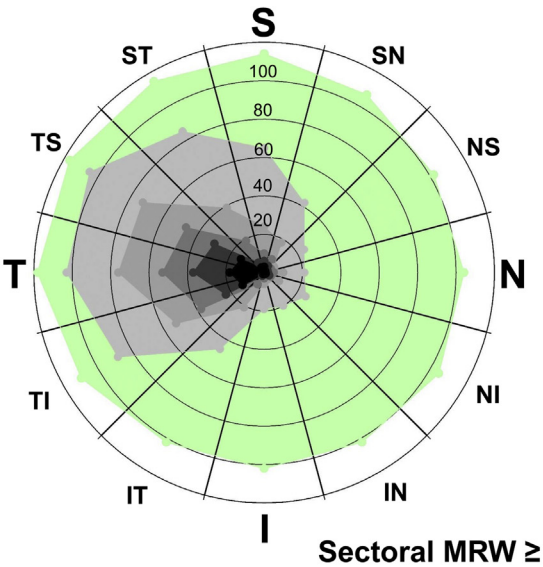

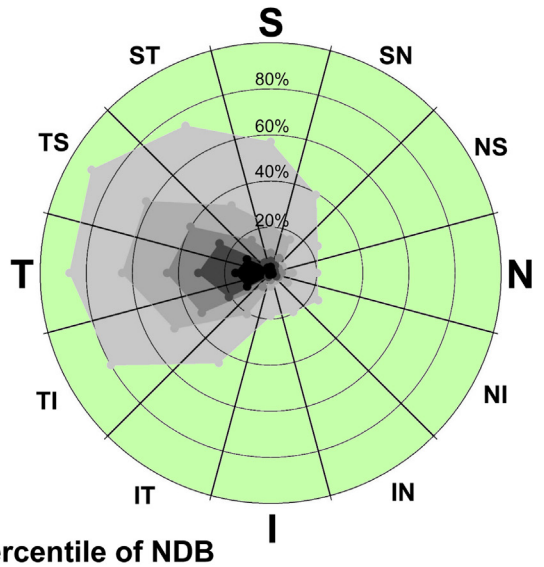

Sectoral MRW ≥ 5th percentile of NDB

Sectoral Frequency of Normal OCT MRW Rim Tissue and its False-Positive Determination
(Number of Normal Eyes)

Sectoral Frequency of Clinician False-Positive Determination of Normal OCT MRW Rim Tissue
(Percent of Normal Eyes)

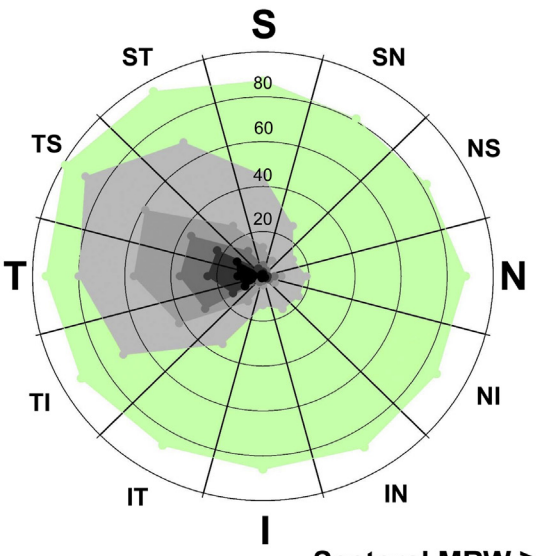

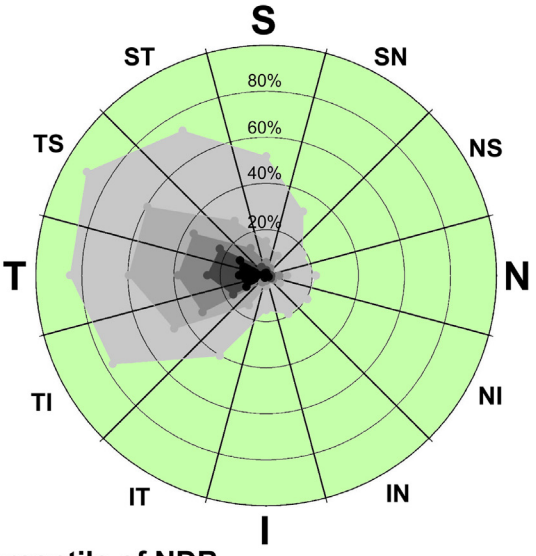

Sectoral MRW ≥ 10th percentile of NDB

Sectoral Frequency of Normal OCT MRW Rim Tissue and its False-Positive Determination
(Number of Normal Eyes)

Sectoral Frequency of Clinician False-Positive Determination of Normal OCT MRW Rim Tissue
(Percent of Normal Eyes)

or % of Eyes with OCT MRW ≥ 5th or ≥ 10th percentile of the NDB
or % of Eyes with CDR ≥ 0.7 by ≥ 1 clinician
or % of Eyes with CDR ≥ 0.7 by ≥ 2 clinicians
or % of Eyes with CDR ≥ 0.7 by ≥ 3 clinicians
or % of Eyes with CDR ≥ 0.7 by ≥ 4 clinicians
or % of Eyes with CDR ≥ 0.7 by all 5 clinicians

Sectoral Frequency of OCT MRW Normal Rim Tissue and the False-Positive Determination of Rim Thinning by Clinicians
(Clinician Detection Criteria CDR ≥ 0.7)

within the inferior-nasal and nasal-inferior sectors, where disc margin–vs-BMO discordance was minimal.

The overall frequency of false-positive determination of suspicious rim thickness is reported for CDR criterion ≥0.7 in Figure 7 and CDR criterion ≥0.6 in Supplemental Figure 4 (Supplemental Material available at AJO.com). Among the 1298 sectors with OCT MRW above the 5th percentile of the NDB, all 5 clinicians' CDR equivalent was ≥0.7 in 4% and all 5 clinicians' CDR equivalent was ≥0.6 in 18%. Among the 1065 sectors with MRW above the 10th percentile of the NDB, all 5 clinicians' CDR equivalent was ≥0.7 in 3% and all 5 clinicians' CDR equivalent was ≥0.6 in 15%.

The sectoral frequency of clinician "false-positive" determination of suspicious rim thickness is reported for a CDR criterion of ≥0.7 in Figure 8 and for CDR criterion ≥0.6 in Supplemental Figure 5 (Supplemental Material available at AJO.com). In sectors with OCT MRW ≥ the 5th percentile of the NDB distribution, the sectoral frequency of all 5 clinicians' CDR being ≥0.7 ranged from 0% to 15% and the sectoral frequency of all 5 clinicians' CDR being ≥0.6 ranged from 0 to 41%. In sectors with OCT MRW ≥ the 10th percentile of the NDB distribution, the sectoral frequency of all 5 clinicians' CDR being ≥0.7 ranged from 0 to 13% and the sectoral frequency of all 5 clinicians' CDR being ≥0.6 ranged from 0 to 36%. For both definitions of normal, and for both detection criteria, false-positive determinations occurred most frequently within the temporal sectors ($P < .001$). A representative study eye demonstrating the false-positive determination of rim thinning temporally and inferiorly is shown in Figure 9.

The Supplemental Table (Supplemental Material available at AJO.com) reports the overall mean sensitivity and specificity of the 5 clinicians using CDR equivalents of 0.6, 0.7, 0.8, and 0.9 as detection criteria for all suspicious sectors. These data demonstrate that for these 5 clinicians, specificities of ≥90% in all sectors were only achieved using a CDR equivalent ≥0.9, but at unacceptably low levels of sensitivity. Sensitivities of ≥90% were only achieved using a CDR equivalent ≥0.6 within the temporal sectors, but at unacceptably low levels of specificity. These data led us to emphasize our findings using the CDR ≥ 0.7 detection criterion, rather than the CDR ≥ 0.6 criterion throughout this report.

DISCUSSION

IN OUR COHORT OF GLAUCOMA AND GLAUCOMA SUSPECT eyes, clinicians most commonly failed to detect OCT suspicious rim thickness nasally, where suspicious rim tissues were common and clinician-vs-OCT rim width discordance was greatest. To the best of our knowledge, no other study has compared glaucoma specialists' sectoral rim width assessments to co-localized OCT MRW measurements or directly assessed clinicians' ability to detect rim tissues that were thin or normal by OCT criteria. Doing so also allowed us to detect that clinicians false-positively determined rim tissue to be thin most commonly in the temporal sectors and to provide OCT anatomic insight into the causes of clinician-vs-OCT rim width discordance. To this point specifically, most eyes demonstrated regions of BMO that were either outside or inside of all 5 clinicians' disc margins (suggesting BMO was clinically invisible to the clinicians), and the frequency of this discordance was greatest for BMO being inside of the clinician disc margins within the temporal sectors. Finally, the specificity of clinician detection of OCT rim thinning only achieved levels ≥90% when CDR ≥ 0.8 or CDR ≥ 0.9 was used, which resulted in unacceptably low sensitivity.

Our finding that OCT suspicious rim tissue occurred as commonly within the nasal sectors as the inferior temporal sectors, and less commonly within the superior temporal sectors, challenges the commonly held notion that the inferior temporal and superior temporal regions of the ONH are most susceptible to glaucomatous damage and are also therefore the first to show damage early in the disease.[23–26] The frequency of nasal rim loss is important because current automated visual field testing does not meaningfully test the retinal areas that correspond to the nasal rim and RNFL and is therefore insensitive to the loss of retinal ganglion cells that correspond to damage within these areas. In a study of 40 healthy, 41 ocular hypertensive, 50 preperimetric, and 50 perimetric glaucoma eyes, Gmeiner and associates reported frequent nasal rim thinning using OCT MRW criteria within all 3 study groups.[12] Leung and associates reported longitudinal RNFL progression to be most common within the inferior temporal clock hours in 116 eyes from 64 glaucoma subjects; however, they also found that progression within the nasal clock hours was only slightly less common in the same eyes.[27]

FIGURE 8. Frequency of optical coherence tomography (OCT) minimum rim width (MRW) "*normal*" rim tissue among the 151 study eyes by fovea–Bruch membrane opening (FoBMO) sector and the frequency and agreement of false-positive determination of rim thinning by clinicians using a cup-to-disc ratio (CDR) criterion of ≥ 0.7. (Upper left) The outermost area (green) represents the number of study eyes in which OCT MRW is *normal* (≥the 5th percentile of the normal database [NDB]) for each sector. Each shade of gray represents the number of normal eyes in which the corresponding number of clinicians' CDR was ≥0.7 (ie, their agreement). (Upper right) The outermost green area denotes 100% of the normal eyes in each sector. Each shade of gray represents the percentage of normal eyes in which the corresponding number of clinicians' CDR was ≥0.7 (ie, their agreement). (Lower left and right) Same as above, except the criteria for "normal" is ≥ the 10th percentile of the NDB for each sector. Taken together, these data suggest that the frequency of OCT MRW normal rim tissue was greatest within the superior-temporal sectors, which is also where the clinicians' false-positive determination of OCT MRW normal rim tissue was highest at all levels of clinician agreement.

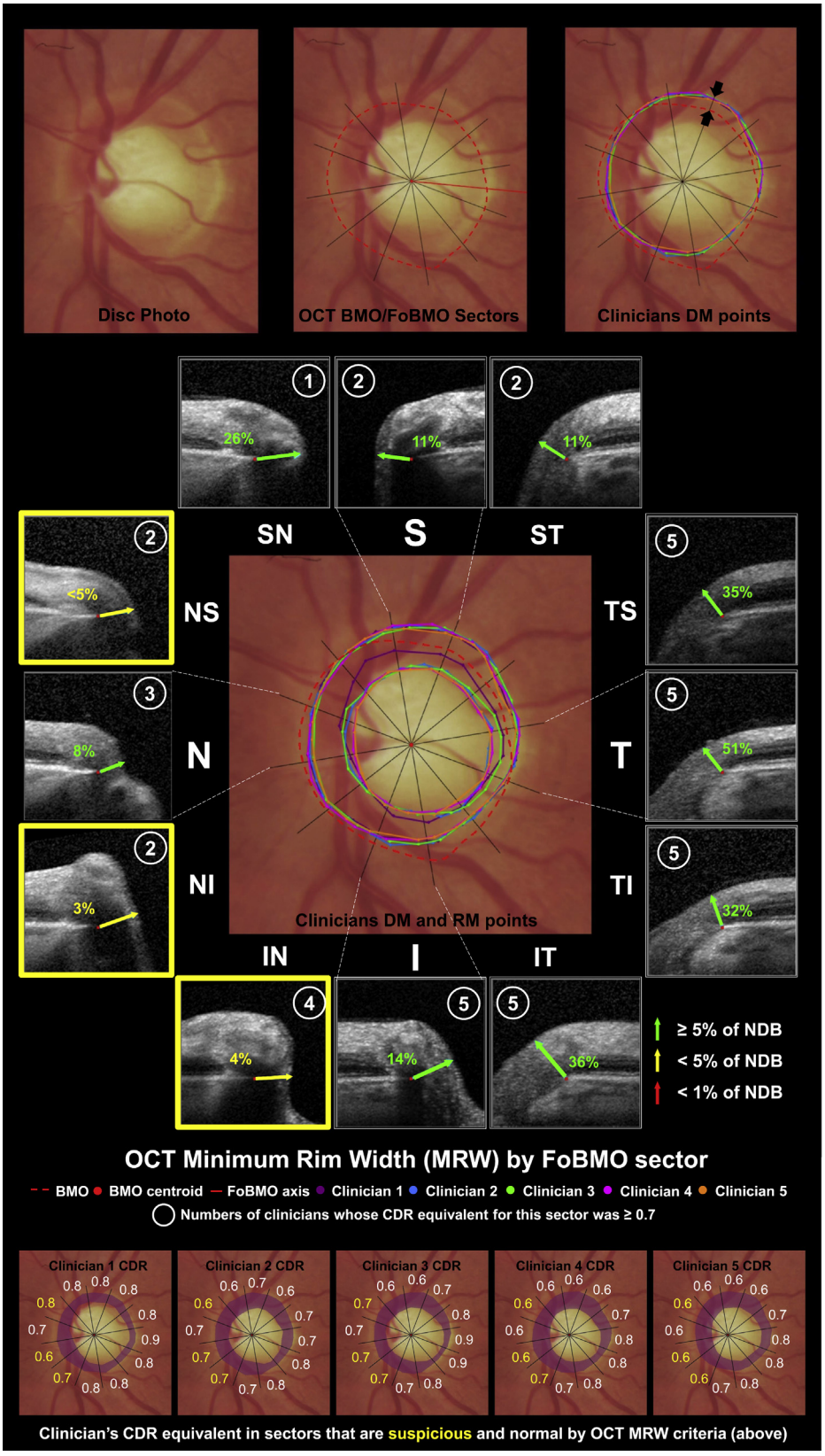
Disc Photo
OCT BMO/FoBMO Sectors
Clinicians DM points
SN
S
ST
NS
TS
N
T
NI
TI
IN
I
IT
26%
11%
11%
<5%
35%
8%
51%
3%
32%
4%
14%
36%
Clinicians DM and RM points
≥ 5% of NDB
< 5% of NDB
< 1% of NDB
OCT Minimum Rim Width (MRW) by FoBMO sector
BMO BMO centroid FoBMO axis Clinician 1 Clinician 2 Clinician 3 Clinician 4 Clinician 5
Numbers of clinicians whose CDR equivalent for this sector was ≥ 0.7
Clinician 1 CDR
Clinician 2 CDR
Clinician 3 CDR
Clinician 4 CDR
Clinician 5 CDR
Clinician's CDR equivalent in sectors that are suspicious and normal by OCT MRW criteria (above)

Reis and associates first described the phenomenon of clinically invisible BMO being "inside" or "outside" of the clinically visible disc margin in 30 glaucoma and 10 healthy control subjects.[28] In the current study, BMO was most commonly (27% of eyes) "outside" all 5 clinicians' disc margins in the nasal sector, and it was most commonly (68% of eyes) "inside" all 5 clinicians' disc margins within the superior-temporal sector (Figures 6, 9, and 10). We propose that in this study BMO is suspicious for being "clinically invisible" within regions of a given eye when all 5 clinicians marked the disc margin "inside" or "outside" of BMO. However, because identifying regions of clinically invisible BMO was not a primary goal of this study, and because we did not specifically ask the clinicians to identify the innermost hyperreflective boundary of the rim tissues as their disc margin (Figure 10), our results only indirectly address this issue. With these limitations, our data confirm the findings of the Reis and associates' study[10] and expand them to 5 clinicians and 151 study eyes.

The fact that the mean rim width for 4 out of the 5 clinicians was greater than the mean OCT MRW in all sectors (Figure 3) confirms the predictions of a second study by Reis and associates,[10] which suggested that clinicians' rim width measurements would most commonly be larger than OCT-based minimum rim width estimates made from BMO, owing to anatomic and geometric differences that were inherent to each form of rim measurement (Figure 10). The geometric difference between the "plane" of clinical estimation (roughly parallel to the retina) and the "plane" of the OCT MRW measurement (perpendicular to the ILM) predisposes the clinical estimate to be greater than the OCT MRW measurement in most circumstances (Figure 10). However, the anatomic components of clinical rim width estimation (disc margin vs BMO discordance and rim margin variability)[6] lead clinicians to overestimate or underestimate the width of the rim tissues within the "clinical" (ie, retinal) plane of estimation, independent of these geometric concerns. To our surprise, we found instances in which all 5 clinicians assigned a rim margin that did not have a clear OCT anatomic foundation and was profoundly different from the ILM (Figure 10), a finding that was not modeled in Reis and associates' study.[10]

The fact that Clinician 1's rim width determinations demonstrate a different relationship to OCT MRW compared to the other 4 clinicians may be related to Clinician 1's having had the greatest exposure to histologic and OCT studies of ONH anatomy prior to the performance of this study. Clinician 1's rim width was greater than OCT MRW in only 44% of sectors, compared to 72%–91% for the other 4 clinicians. However, while this translated to a higher sensitivity to OCT MRW suspicious rim tissue detection using the CDR ≥ 0.7 criterion (72% of all suspicious sectors, compared to a range of 40%–56% for the other 4 clinicians), it also yielded a higher rate of false-positive rim thinning detection using MRW ≥ 10% of the NDB criteria (41%, compared to 8%–20% for the others).

While there are no other studies that have directly compared clinicians' sectoral rim width assessments to co-localized OCT MRW measurements, there are many studies comparing clinicians' CDRs to OCT-derived CDRs.[29–33] In the most recent of these, Mwanza and associates[33] compared vertical and horizontal CDR measurements of 2 glaucoma specialists in 195 glaucoma and glaucoma suspect eyes and reported poor agreement between the clinician and OCT values, with OCT CDRs being greater than the clinicians' CDRs. This CDR result is compatible with the finding that clinician rim width estimates were on average larger than OCT MRW measurements in our study eyes.

In the present study, in addition to the fact that OCT MRW suspicious rim tissues most commonly occurred in the nasal sectors, clinicians most commonly failed to detect them there. This finding, combined with those of others,[12,27] strongly suggests that there is a need to improve the clinical examination of the nasal ONH for the detection of both glaucoma and its progression. We believe that the goal of these efforts should be to improve the sensitivity and specificity of their ability to detect OCT suspicious rim tissue rather than to make clinicians' rim width estimation equal to OCT MRW. However, to do so, we propose that characterizing the anatomic causes

FIGURE 9. Clinician false-positive determination of rim thinning temporally and inferiorly in a representative study eye using a cup-to-disc ratio (CDR) ≥ 0.7 criterion. (Top left) Fundus photograph from study subject DIS413. (Top center) Bruch membrane opening (BMO), the centroid of BMO, the fovea–BMO axis (FoBMO axis, red line), and the 12 FoBMO 30-degree (clock-hour) sectors (black lines). (Top right) BMO relative to the disc margin points of all 5 clinicians. Note that BMO is well inside the clinical disc margin points of all 5 clinicians superiorly and superior-temporally (black arrows), suggesting that BMO is clinically invisible to these clinicians in this region.[10,23] (Center panels) BMO and each clinician's disc margin and rim margin points have been superimposed on the fundus photograph in the center, and optical coherence tomography (OCT) rim anatomy along with its quantification relative to a Caucasian normative database (NDB) are shown for each FoBMO sector. Note that in the inferior (I), inferior-temporal (IT), temporal-inferior (TI), temporal (T), and temporal-superior (TS) sectors, all 5 clinicians are suspicious for rim thinning by CDR criterion ≥ 0.7 in sectors in which the OCT minimum rim width (MRW) values are > the 20th percentile of the NDB. Note also the variable levels of clinician detection of OCT MRW suspicious rim thickness within the nasal-superior, nasal-inferior, and inferior-nasal sectors. In a white circle at the top of each OCT anatomy box, the number of clinicians that were suspicious for rim thinning by CDR ≥ 0.7 criterion are noted. (Bottom row) Each clinician's rim width (purple) and their CDR equivalent for the OCT MRW *suspicious* sectors are shown. See Figure 10 for a more detailed discussion of the inferior-temporal sector anatomy.

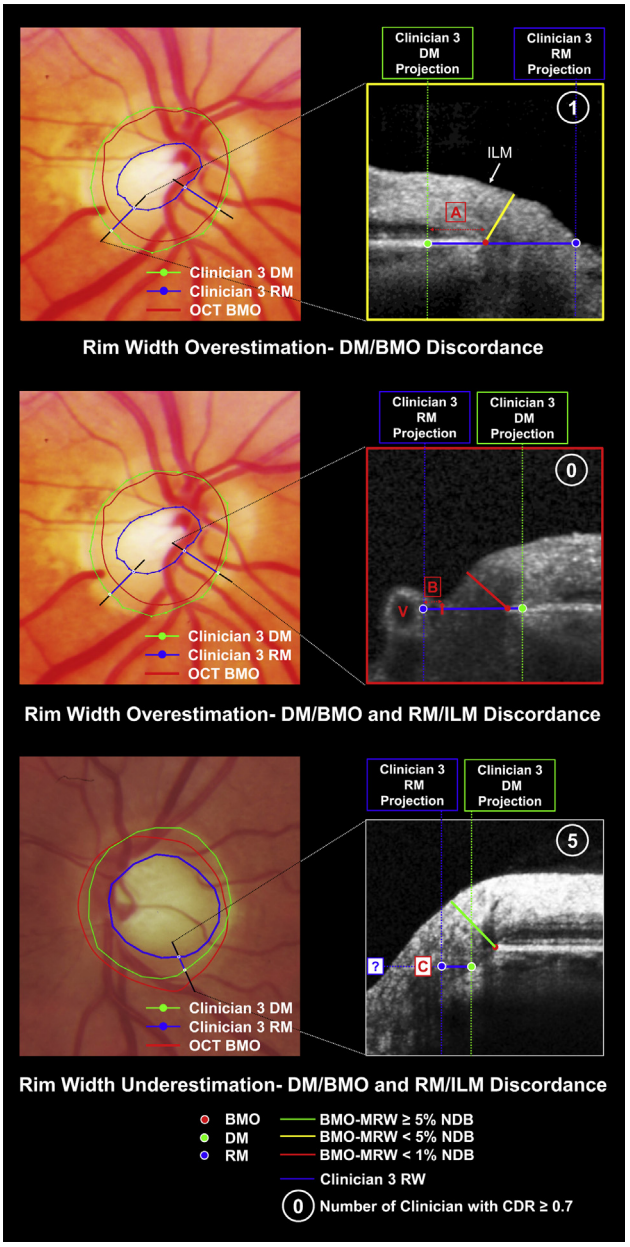

FIGURE 10. While clinician rim width is predisposed to be larger than optical coherence tomography (OCT) minimum rim width (MRW) by geometry alone, the anatomic components of clinician rim width estimation produce rim width overestimation or rim width underestimation within the clinician's plane of reference, that are separate from the geometric effects. (Top left) Color photograph of study eye DIS132 (from Figure 6) showing Clinician 3's disc margin (DM; green) and rim margin (RM; blue) points relative to OCT Bruch membrane opening (BMO; red) and the *inferior-temporal* location of the cropped OCT B-scan shown in the top right panel. (Top right) OCT BMO and the projection of clinicians' DM and RM points are displayed. The "*geometric*" difference between the clinical use of a "retinal" plane for rim estimation (Clinician 3's rim width estimate; blue line) and an OCT MRW measurement (yellow) predispose the clinical rim width estimate to be larger than the OCT MRW measurement. However, at least 2 additional anatomic influences can lead to clinician overestimation (Top right and Center right panels) or underestimation (Bottom right panel) of rim width within the "horizontal" clinical plane of estimation. The first is OCT BMO vs clinical DM discordance (A), which at this location further increases the clinical rim width measurement. The second is clinical RM vs internal limiting membrane (ILM) discordance, which is illustrated in center and bottom panels. (Center left) Similar to the top left panel, but shows the *inferior-nasal* location of the cropped OCT B-scan shown in center right panel, in which there is DM vs OCT BMO discordance (smaller than *inferior-temporally*, above) but also RM vs ILM discordance (B), likely owing to the presence of a vessel (v) that obscures the clinician's view of the ILM. In both of these locations (Top right and Center right panels), overestimation of the rim width within the retinal plane underlies the low number of clinicians (circled number in upper right corner of each panel) that detected rim tissues that were thin by OCT. (Bottom left) Similar to top panels, but showing study eye DIS413 (from Figure 9), and the *inferior-temporal* location of the B-scan shown in the bottom right panel. (Bottom right) In this sector, there is DM vs BMO discordance that is likely related to the externally oblique border tissues,[10,23] and profound RM vs ILM discordance (C), the underlying reasons for which are not clear. Why none of the 5 clinicians was able to discern the ILM (?) in this location (clinical RMs are similar here in Figure 9) warrants further study. Underestimation of rim tissue thickness within the retinal estimating plane in this location underlies the fact that all 5 clinicians determined rim tissues to be suspicious that were normal by OCT.

of disc margin and rim margin discordance will be necessary (Figure 10) and that integrating what is learned into clinical disc examination instruction will eventually improve clinician performance. Studies to test these hypotheses are necessary.

Our study is limited by the small number of clinician examiners. However, 5 clinicians is equal to or exceeds the number of examiners in most previous studies,[29–33] and their range of training and experience is likely similar to most tertiary care glaucoma services. Our study is also limited by the fact that it only assessed the ability of a clinical rim width estimate to detect rim tissues that were suspicious for being thin by OCT criteria. We focused on disc margin and rim width estimation because these components of the clinical examination could be quantified and compared to OCT rim anatomy. We did not directly compare clinician rim margin to OCT MRW rim margin assessment because of the geometric differences that are inherent to the 2 measurement strategies. Whether the OCT MRW rim margin can be or should be a target for clinician rim margin assignment is of interest but is beyond the scope of this report. We also did not ask the clinicians if each disc sector was suspicious for glaucoma and did not allow them to include other aspects of the clinical examination, such as pallor, nerve fiber layer thinning, and nerve fiber layer

hemorrhages. We only assessed glaucoma specialists. How their performance compares to general ophthalmologists and optometrists and whether the clinical examination of all clinicians can be improved through OCT-based instruction deserve further study.

Finally, it is also worth noting that while 1 clinician was in glaucoma fellowship training during the study and a second was an early-career visiting clinician-scientist from China, neither of these clinicians (Clinicians 2 and 4, respectively) were outliers when compared to Clinicians 1 and 5. Our study was not designed to demonstrate the effect of practice duration on clinician performance. Such a study would require multiple clinicians at each level of experience over the full duration of an average career and include a nonlinear assessment of the post-fellowship learning curve. These kinds of analyses are beyond the scope of the present report.

In summary, in glaucoma and glaucoma suspect eyes, clinicians commonly failed to detect OCT suspicious rim thickness in all ONH sectors, but most frequently nasally, where suspicious rim tissues were also most common and clinician-vs-OCT rim width discordance was greatest. Clinicians falsely determined the rim to be thin most frequently in the temporal sectors, where regions that were suspicious for demonstrating clinically invisible BMO were also most common. Clinician rim width estimates were consistently larger than OCT MRW measurements for 4 of the 5 clinicians, and the difference between the 2 was greatest in the nasal sectors. We propose that the incorporation of sectoral OCT rim anatomy and its quantification into the clinical disc examination, and its instruction, may be necessary to improve clinician rim width estimation, especially within the nasal sectors of the ONH.

FUNDING/SUPPORT: NIH/NEI R01-EY-019674; NIH/NEI R01-EY021281; LEGACY GOOD SAMARITAN FOUNDATION, PORTLAND, Oregon, USA; Heidelberg Engineering, GmbH, Heidelberg, Germany. The listed sponsors/funding organizations had no role in the design, conduct, analysis, or reporting of this research. Financial Disclosures: Robert M. Kinast: Allergan, Ocular Therapeutix. Steven L. Mansberger: Consultant: Envisia, Santen, Gore, Aerie. Claude F. Burgoyne is a consultant to Heidelberg Engineering. In this role, he receives unrestricted research support, instruments, software, occasional travel support, but no honorarium or personal income. The following authors have no financial disclosures: Seung Woo Hong, Helen Koenigsman, Hongli Yang, Ruojin Ren, Juan Reynaud, Brad Fortune, Shaban Demirel, and Stuart K. Gardiner. All authors attest that they meet the current ICMJE criteria for authorship.

REFERENCES

1. Varma R, Steinmann WC, Scott IU. Expert agreement in evaluating the optic disc for glaucoma. *Ophthalmology* 1992; 99(2):215–221.
2. Klein BE, Magli YL, Richie KA, Moss SE, Meuer SM, Klein R. Quantitation of optic disc cupping. *Ophthalmology* 1985; 92(12):1654–1656.
3. Lichter PR. Variability of expert observers in evaluating the optic disc. *Trans Am Ophthalmol Soc* 1976;74:532–572.
4. Varma R, Spaeth GL, Steinmann WC, Katz LJ. Agreement between clinicians and an image analyzer in estimating cup-to-disc ratios. *Arch Ophthalmol* 1989;107(4):526–529.
5. Jampel HD, Friedman D, Quigley H, et al. Agreement among glaucoma specialists in assessing progressive disc changes from photographs in open-angle glaucoma patients. *Am J Ophthalmol* 2009;147(1):39–44 e31.
6. Hong SW, Koenigsman H, Ren R, et al. Glaucoma specialist optic disc margin, rim margin and rim width discordance in glaucoma and glaucoma suspect eyes. *Am J Ophthalmol* 2018;192:65–76.
7. He L, Ren R, Yang H, et al. Anatomic vs. acquired image frame discordance in spectral domain optical coherence tomography minimum rim measurements. *PLoS One* 2014;9(3):e92225.
8. Chauhan BC, Burgoyne CF. From clinical examination of the optic disc to clinical assessment of the optic nerve head: a paradigm change. *Am J Ophthalmol* 2013;156(2):218–227.e212.
9. Chauhan BC, Danthurebandara VM, Sharpe GP, et al. Bruch's membrane opening minimum rim width and retinal nerve fiber layer thickness in a normal white population: a multicenter study. *Ophthalmology* 2015;122(9):1786–1794.
10. Reis AS, O'Leary N, Yang H, et al. Influence of clinically invisible, but optical coherence tomography detected, optic disc margin anatomy on neuroretinal rim evaluation. *Invest Ophthalmol Vis Sci* 2012;53(4):1852–1860.
11. Chauhan BC, O'Leary N, AlMobarak FA, et al. Enhanced detection of open-angle glaucoma with an anatomically accurate optical coherence tomography-derived neuroretinal rim parameter. *Ophthalmology* 2013;120(3):535–543.
12. Gmeiner JM, Schrems WA, Mardin CY, Laemmer R, Kruse FE, Schrems-Hoesl LM. Comparison of Bruch's membrane opening minimum rim width and peripapillary retinal nerve fiber layer thickness in early glaucoma assessment. *Invest Ophthalmol Vis Sci* 2016;57(9):OCT575–OCT584.
13. Wollstein G, Garway-Heath DF, Fontana L, Hitchings RA. Identifying early glaucomatous changes. Comparison between expert clinical assessment of optic disc photographs and confocal scanning ophthalmoscopy. *Ophthalmology* 2000;107(12):2272–2277.
14. Reus NJ, Lemij HG, Garway-Heath DF, et al. Clinical assessment of stereoscopic optic disc photographs for glaucoma: the European Optic Disc Assessment Trial. *Ophthalmology* 2010; 117(4):717–723.
15. Gardiner SK, Johnson CA, Demirel S. Factors predicting the rate of functional progression in early and suspected glaucoma. *Invest Ophthalmol Vis Sci* 2012;53(7):3598–3604.
16. Strouthidis NG, Yang H, Reynaud JF, et al. Comparison of clinical and spectral domain optical coherence tomography

optic disc margin anatomy. *Invest Ophthalmol Vis Sci* 2009; 50(10):4709–4718.
17. Iwase A, Sawaguchi S, Sakai H, Tanaka K, Tsutsumi T, Araie M. Optic disc, rim and peripapillary chorioretinal atrophy in normal Japanese eyes: the Kumejima Study. *Jpn J Ophthalmol* 2017;61(3):223–229.
18. Iwase A, Suzuki Y, Araie M, et al. The prevalence of primary open-angle glaucoma in Japanese: the Tajimi Study. *Ophthalmology* 2004;111(9):1641–1648.
19. Bokman CL, Pasquale LR, Parrish RK 2nd, Lee RK. Glaucoma screening in the Haitian Afro-Caribbean population of South Florida. *PLoS One* 2014;9(12):e115942.
20. Kim CS, Seong GJ, Lee NH, Song KC, Namil Study Group, Korean Glaucoma Society. Prevalence of primary open-angle glaucoma in central South Korea the Namil study. *Ophthalmology* 2011;118(6):1024–1030.
21. Gupta P, Zhao D, Guallar E, Ko F, Boland MV, Friedman DS. Prevalence of glaucoma in the United States: The 2005-2008 National Health and Nutrition Examination Survey. *Invest Ophthalmol Vis Sci* 2016;57(6):2905–2913.
22. Ashaye A, Ashaolu O, Komolafe O, et al. Prevalence and types of glaucoma among an indigenous African population in southwestern Nigeria. *Invest Ophthalmol Vis Sci* 2013; 54(12):7410–7416.
23. See JL, Nicolela MT, Chauhan BC. Rates of neuroretinal rim and peripapillary atrophy area change: a comparative study of glaucoma patients and normal controls. *Ophthalmology* 2009; 116(5):840–847.
24. Quigley HA, Addicks EM, Green WR. Optic nerve damage in human glaucoma. III. Quantitative correlation of nerve fiber loss and visual field defect in glaucoma, ischemic neuropathy, papilledema, and toxic neuropathy. *Arch Ophthalmol* 1982;100(1):135–146.
25. Hood DC, De Moraes CG. Challenges to the common clinical paradigm for diagnosis of glaucomatous damage with OCT and visual fields. *Invest Ophthalmol Vis Sci* 2018;59(2): 788–791.
26. Quigley HA, Green WR. The histology of human glaucoma cupping and optic nerve damage: clinicopathologic correlation in 21 eyes. *Ophthalmology* 1979;86(10):1803–1830.
27. Leung CK, Cheung CY, Weinreb RN, et al. Evaluation of retinal nerve fiber layer progression in glaucoma: a study on optical coherence tomography guided progression analysis. *Invest Ophthalmol Vis Sci* 2010;51(1):217–222.
28. Reis AS, Sharpe GP, Yang H, Nicolela MT, Burgoyne CF, Chauhan BC. Optic disc margin anatomy in patients with glaucoma and normal controls with spectral domain optical coherence tomography. *Ophthalmology* 2012;119(4): 738–747.
29. Arnalich-Montiel F, Munoz-Negrete FJ, Rebolleda G, Sales-Sanz M, Cabarga C. Cup-to-disc ratio: agreement between slit-lamp indirect ophthalmoscopic estimation and stratus optical coherence tomography measurement. *Eye (Lond)* 2007; 21(8):1041–1049.
30. Hatch WV, Trope GE, Buys YM, Macken P, Etchells EE, Flanagan JG. Agreement in assessing glaucomatous discs in a clinical teaching setting with stereoscopic disc photographs, planimetry, and laser scanning tomography. *J Glaucoma* 1999; 8(2):99–104.
31. Kotera Y, Yasuno Y, Hangai M, et al. Comparison of spectral domain optical coherence tomography and color photographic imaging of the optic nerve head in management of glaucoma. *Ophthalmic Surg Lasers Imaging* 2009;40(3): 255–263.
32. Savini G, Espana EM, Acosta AC, Carbonelli M, Bellusci C, Barboni P. Agreement between optical coherence tomography and digital stereophotography in vertical cup-to-disc ratio measurement. *Graefes Arch Clin Exp Ophthalmol* 2009; 247(3):377–383.
33. Mwanza JC, Huang LY, Budenz DL, Shi W, Huang G, Lee RK. Differences in optical coherence tomography assessment of Bruch membrane opening compared to stereoscopic photography for estimating cup-to-disc ratio. *Am J Ophthalmol* 2017;184:34–41.